Thermal expansion behavior of holes in graphene nanomeshes

Newton C. B. Mostério[1] and Alexandre F. Fonseca[2,*]

[1]*Programa de Pós-graduação em Engenharia Metalúrgica – Escola de Engenharia Industrial e Metalúrgica de Volta Redonda (EEIMVR) – UFF, Av. dos Trabalhadores, 420, Volta Redonda, RJ, 27255-125, Brazil*

[2]*Applied Physics Department, State University of Campinas, Campinas-SP, Sao Paulo, Brazil*

(Received 10 February 2014; revised manuscript received 27 March 2014; published 23 May 2014)

The thermal expansion of a hole, in a planar system, follows the same trend as the thermal expansion of the whole system, i.e., the hole expands (contracts) if the material expands (contracts) under thermal excitation. At nanoscale, this phenomenon has not been studied so far. Here, using tools of classical molecular dynamics simulations, we show that graphene nanomeshes (GNMs) behave oppositely: While the whole structure contracts (expands), the nanoholes expand (contract) under thermal excitation. We propose and test a simple mechanism to describe this unexpected behavior in terms of out-of-plane vibrations of the atoms close to and far from the edges of the holes. This mechanism allows us to see that, contrary to usual planar systems, this behavior comes from nonuniform thermal expansion along the structure. Although the thermal expansion of holes in GNMs is contrary to the classical prediction, we verify that the thermal expansion of the whole GNM structure is the same as that of pristine graphene.

DOI: 10.1103/PhysRevB.89.195437 PACS number(s): 65.80.Ck, 62.23.Kn, 65.40.De

I. INTRODUCTION

A very common experience is pouring hot water over a tight metal lid of a glass jar to easily open it. The contact forces between the lid and the jar decrease because the thermal expansion of the metal lid is larger than that of the glass. But the difference in the coefficients of thermal expansion between the metal and the glass is not the only physical phenomenon behind this simple experience. Because the metal lid has the shape of a short hollow cylinder with one side open, another phenomenon, and one of the most interesting problems in thermal physics, also happens: *the thermal expansion of a hole*. As can be found in any textbook of thermal physics (see, for example, Ref. [1]), the holes follow exactly the thermal expansion behavior of the material, i.e., if the material expands (contracts) under thermal excitation, the holes within it expand (contract). Otherwise, it would not be easy to open the jar. The explanation for this phenomenon is quite simple. As the thermal expansion of the material is *uniform* along the structure, the hole edges will expand according to the expansion of the material. This phenomenon has practical applications as, for example, the shrink-fitting method used to join two or more pieces of an engine, expansion joints in bridges or pipes, and in riveting steel or aluminum plates in large buildings and aircrafts.

At nanoscale, many systems can exhibit unusual or counterintuitive behaviors. Examples are the increase in Young's modulus of nanowires of diameters smaller than 70 nm [2], unusual electron-phonon interactions and mechanical properties of metal nanoparticles [3], existence of "exotic" metallic structures [4], auxeticity in buckypapers [5], violation of universal behavior in spatial conformations of one-atom thick nanostructures [6], and, speaking of thermal expansion, the negative thermal expansion of graphene [7–10].

The extraction of an individual layer of graphite, or *graphene*, was considered a great achievement by the scientific community [11–13]. After a decade of intensive research, the remarkable physical properties of graphene continue motivating the development of new, fast, and more efficient graphene-based applications [14]. However, because the absence of band gap limits the application of graphene to nanoelectronics, scientists started looking at some derivatives of graphene that possess nonzero band gap. The most common examples of such derivatives are graphene nanoribbons [15,16], graphane [17], and graphene oxide [18]. A few years ago, a new nonzero band gap derivative of graphene structure, called *graphene nanomesh* (GNM), was synthesized by different methods: block copolymer lithography [19], self-assembled monolayers of colloidal microspheres [20], photocatalytic patterning [21], and other methods [22–25]. Basically, a GNM is a graphene structure with a periodic array of holes of different sizes and hole-to-hole, or *neck*, distances. Potential applications for GNMs are chemical sensing, supercapacitors, DNA sequencing, photothermal therapy, among others [23,26–29].

While the few theoretical works on GNMs have focused on their electronic [30–34] and mechanical properties [35–37], to our knowledge, only a few have investigated thermal properties of GNMs so far [38,39]. In this paper, by performing numerical experiments, we present an interesting observation regarding the thermal expansion behavior of the holes in GNMs. While, as mentioned above, the thermal expansion of a hole usually follows the same trend as the thermal expansion of the material, in GNMs the thermal expansion of the holes behaves oppositely: At certain temperature ranges (including room temperature) they expand (contract) if the structure contracts (expands) under thermal excitation. Inspired by the explanation for the negative values of the thermal expansion of pristine graphene in terms of *out-of-plane vibrations* [40,41], we propose a simple mechanism to explain the thermal expansion of holes in GNMs. An analysis of the movement of the atoms *close to* and *far from* the edges of the holes

*afonseca@ifi.unicamp.br

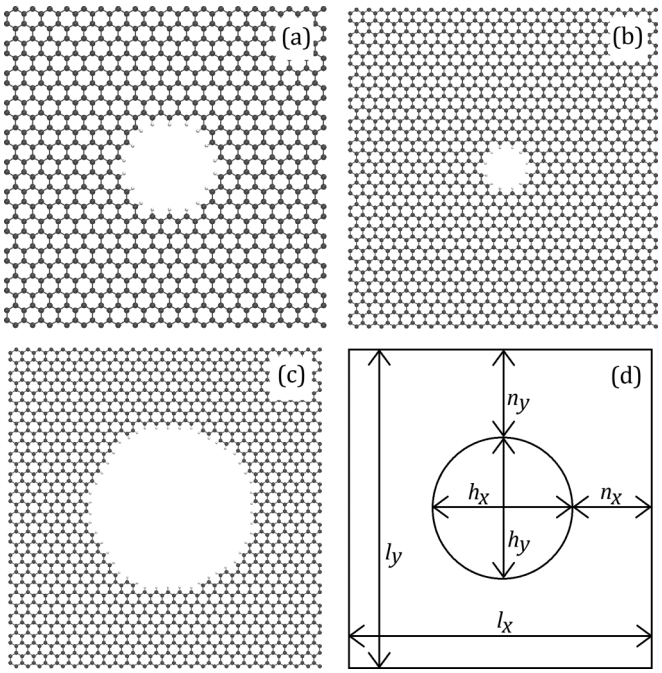

FIG. 1. GNMs considered in the present study. They are named (a) GNM-46, (b) GNM-62, and (c) GNM-67, where the numbers represent the approximated values of the lateral dimensions in angstroms. The holes are passivated with hydrogen. Carbon (hydrogen) atoms are represented by gray (white) spheres. The length of the structure along *zigzag*, l_x, and *armchair*, l_y, directions and x and y dimensions of hole and neck sizes, (h_x,h_y) and (n_x,n_y), respectively, are depicted in (d).

confirms the proposed mechanism and reveals that in GNMs the thermal expansion is not uniform along the structure. Here we describe the GNMs considered in this study, the form of calculation of their *thermal expansion coefficient* (TEC), the computational methods and protocols, and the results.

We have chosen three different GNMs with different hole sizes to investigate the thermal expansion behavior of the holes (see Fig. 1). We labeled them as "GNM-46," "GNM-62," and "GNM-67," where the numbers represent the approximated value (in angstroms) of their lateral dimensions. The approximated values of their hole sizes are 1.5, 1.0, and 3.6 nm, respectively. Figure 1 also shows the meaning of the variables used along the calculations. *Zigzag* and *armchair* directions are defined as x and y, and all x and y variables are projections of the corresponding distances onto the x-y plane. Although theory has predicted independence of the TEC of a plate on its length [42], in the case of graphene, very small structures are not adequate for the study of thermal expansion because it is also known that low frequency acoustic phonons are important to the determination of negative values of the TEC of graphene [40,42,43]. Besides, small structures cannot have nanosize holes and we chose to simulate GNMs having, at least, ∼1 nm of hole size.

In what follows, we will present the theory and computational methods used to calculate the TEC of the GNMs (Sec. II); the results for the TEC of GNMs and their holes, including the calculations of the TEC of pristine graphene for comparison (Sec. III); an analysis of the strange behavior of the TEC of the holes, including the proposal of a scheme to describe the mechanism behind this behavior (Sec. IV); and the summary of the main results of this study (Sec. V).

II. THEORY AND COMPUTATIONAL METHODS

In a solid, the dependence of the thermal expansion with pressure is usually neglected and the TEC (α) is simply given by

$$\alpha_W(T) = \frac{1}{W}\frac{dW}{dT}, \tag{1}$$

where W can be the equilibrium length L, area A, or volume V of the material as functions of the equilibrium temperature T. α_L, α_A, and α_V then represent linear, area, and volume TECs, respectively. Here we will present results for linear and area thermal expansions α_L and α_A, respectively, of the GNMs and their holes and necks. The TEC of the corresponding pristine graphene structures is also shown for comparison.

Tools of classical molecular dynamics (MD) from the LAMMPS package [44,45] were employed in this study, using the well known second generation of the reactive empirical bond order (REBO) potential [46]. REBO is well known to accurately describe carbon-carbon interactions and has been extensively used to study the physical properties of carbon structures [47–52]. It also has been used to calculate the TEC of graphene [53] and carbon nanotubes [54]. Here we first tested our protocols of simulations estimating the TEC of graphene with the REBO potential. Our results (shown in the next section) are compatible with both experimental [8–10] and theoretical [40,55] values for the TEC of graphene. Also, in a conference paper [36], we have reported the TEC of some GNMs obtained from MD simulations using REBO, whose values are of the same order of magnitude of both experimental and theoretical values of the TEC of graphene. In this section we will present the protocols of simulations and the form of calculation of the TEC of the structures. The results will be presented in the next section.

A. Protocols of molecular dynamics simulations

The MD simulations were performed within the NPT ensemble (constant number of atoms, pressure, and temperature) using periodic boundary conditions along x and y directions, allowing the l_x and l_y box sizes (see Fig. 1) to be relaxed together with the structure. l_{x0} and l_{y0} are the equilibrium values of the box sizes of the structure. They were recorded for each value of temperature from the list below. The set of values of l_{x0} and l_{y0} were used, later, to obtain the functions $l_{x0}(T)$ and $l_{y0}(T)$. The Newton's equations of motion were integrated with the velocity-Verlet integrator with the time step of 0.5 fs, for a total of 3 900 000 steps (or 1.95 ns) to ensure full equilibration of the structure and the box sizes. 100 000 steps (or 50 ps) of simulation were used to smoothly elevate the temperature from the actual to the next value according to the list of temperatures given below. The Nose-Hoover thermostat and barostat were used to fix the temperature and pressure of each simulation. While the pressure was set to zero in all

simulations, the values of temperature considered here were

$$\{50\ \text{K}, 100\ \text{K}, 150\ \text{K}, 200\ \text{K}, 250\ \text{K}, 300\ \text{K}, 350\ \text{K}, 400\ \text{K}, 450\ \text{K}, 500\ \text{K}, 550\ \text{K}, 600\ \text{K}, 700\ \text{K}, 800\ \text{K}, 900\ \text{K}, 1000\ \text{K}\}. \quad (2)$$

One key point in these simulations is the choice of the barostat pressure damping parameter $Pdamp$ (see LAMMPS package [44,45] manual for the details). The choice was made based on a set of previous simulations with pristine graphene. The value $Pdamp = 10$ was chosen because it provided the smallest average value for both the components of the pressure tensor along x and y directions of the structure.

Additional MD simulations within NVT ensemble (constant number of atoms, volume, and temperature) were performed to calculate the average of the hole and neck sizes for the equilibrium structures at every value of temperature listed above. These MD simulations were carried out using periodic boundary conditions along x and y directions, with the box sizes of the structures fixed in their equilibrium values l_{x0} and l_{y0}, as obtained from the previous NPT simulations at each temperature. Here the Newton's equations of motion were integrated with the velocity-Verlet integrator with the time step of 0.5 fs, for about 200 ps, and the temperatures of the structure were simulated by a Nose-Hoover thermostat as implemented in LAMMPS.

The determination of the values of the equilibrium box sizes l_{x0} and l_{y0} was made as follows. Along each MD simulation within NPT ensemble of the GNMs depicted in Fig. 1 at a given value of temperature, the values of l_x and l_y of the box sizes were collected every 100 fs. The equilibrium values of l_{x0} and l_{y0} were then calculated as the average of 19 500 values of l_x and l_y collected along the MD simulation of 1.95 ns. In order to calculate the time average of the hole and neck sizes [the pairs (h_{x0}, h_{y0}) and (n_{x0},n_{y0}), respectively] for each temperature, we collected a frame of the GNM structure every 1 ps of the additional MD simulation of 200 ps within the NVT ensemble, with fixed box sizes at the equilibrium values l_{x0} and l_{y0}.

B. Calculation of the TEC

After calculating the set of equilibrium sizes of the GNM structures and their holes and necks, we fit them to a fourth order polynomial function in T to obtain $l_{x0}(T)$, $l_{y0}(T)$, $h_{x0}(T)$, $h_{y0}(T)$, $n_{x0}(T)$, and $n_{y0}(T)$. Finally, using Eq. (1), we obtain the corresponding linear TECs $\alpha(T)$. This is the same form of calculation of the TEC of graphene used by Bao *et al.* [8]. The areas of the whole structure of the GNM and of its hole are simply defined here as the product of the lateral dimensions, $l_x \times l_y$ and $h_x \times h_y$ [56], respectively. Their area TECs are calculated following the same procedure to calculate the linear TECs.

In the next section we present the results for the TECs of all GNMs and the corresponding graphenes, i.e., the graphene structures with the same size of the GNMs studied here.

III. TECS OF GNM STRUCTURES

In this section we present the results for the TEC of the GNMs structures depicted in Fig. 1. The TECs of the corresponding pristine graphenes are calculated for reference, test of the potential, and analysis of the results.

A. TEC of graphene

Before presenting the results for the TEC of the GNMs, we first present the results of the linear TEC of the graphene in order to validate our computational method and protocols. We considered here graphene structures of the same size of the GNMs. To facilitate the reference, we are going to label the graphene structures of the same sizes of the GNM-46, GNM-62, and GNM-67 as "G-46," "G-62," and "G-67," respectively.

We first show, in Fig. 2, the variations of the equilibrium box sizes l_{x0} and l_{y0} with temperature of the G-67 structure. The forms of variation of l_{x0} and l_{y0} with temperature of the graphene structures G-46 and G-62 are similar to that of G-67 and are not shown. Using Eq. (1) to obtain $\alpha_{lx}(T)$ and $\alpha_{ly}(T)$ from the equilibrium values of box sizes l_{x0} and l_{y0}, and defining the average linear TEC of graphene as $\alpha_L \equiv \frac{1}{2}[\alpha_{lx}(T) + \alpha_{ly}(T)]$, we show in Fig. 3 the linear TEC of G-46, G-62, and G-67 graphene structures.

From Fig. 3 we can see that the values of the TEC of graphene are of the same order of magnitude of the values reported in literature. At 300 K, for example, our results are $\alpha_L \sim -1.6 \times 10^{-6}$ K^{-1}, while α is within the range from ~ -6.0 to -3.5×10^{-6} K^{-1} from theoretical calculations [40,55,57], and from ~ -8 to -7×10^{-6} K^{-1} from experiments [8–10]. Figure 3 also shows that the TEC of graphene depends on the size of the structure, but the difference decreases with the increase of the size.

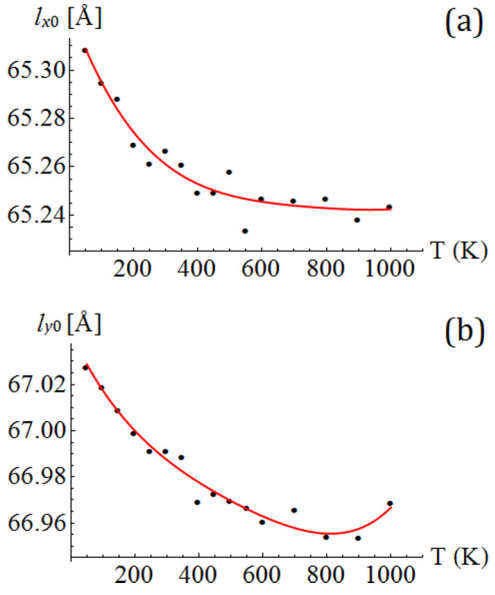

FIG. 2. (Color online) Variation of (a) l_{x0} and (b) l_{y0} with temperature of the G-67 structure. Points are results from MD simulations and the line is the fitting of the points to a fourth order polynomial in T.

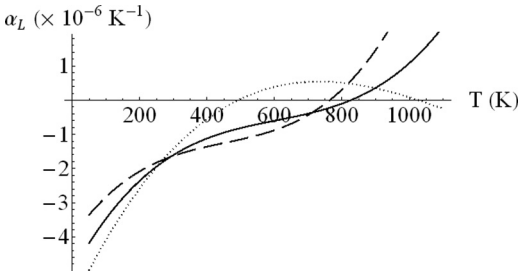

FIG. 3. Linear TECs of pristine graphene structures G-46 (dotted line), G-60 (dashed line), and G-67 (full line).

B. TEC of the GNMs

Figure 4 shows the results for the average ($\alpha_L \equiv \frac{1}{2}\alpha_x + \frac{1}{2}\alpha_y$) linear TECs of the GNMs and their holes and necks. Also, Fig. 4 shows the TEC of the corresponding pristine graphene for comparison. The first observation is that the differences between the TEC of the GNM and that of the corresponding graphene are quite small, at least, for most of the values of temperature. This will be discussed later. For all three GNMs we see regions in temperature where the linear TEC of the whole structure (full line) is negative while the linear TEC of the hole (dashed line) is positive. For the GNM-67, it happens for all values of temperature within the range given by Eq. (2). For the GNM-46, the TEC of the hole is negative for $T <\sim 150$ K and the TEC of the whole structure is positive for $T > \sim 650$ K. For the GNM-62, the TEC of the hole is negative for $T < \sim 250$ K and the TEC of the whole structure is positive for $\sim 560 < T < \sim 860$ K. An important observation is that the TEC of the neck is always negative for all three GNMs. The thermal contraction of the neck is playing an important rule in the determination of the sign of the TEC of the whole structure. It is compensating the thermal expansion of the hole for the temperature values where it is positive. Also, independent of the sign of the TEC of the holes, it is clear from Fig. 4 that the TEC of the necks and holes are very different, what is an unexpected behavior if compared to that of a hole in a plate as predicted by classical physics.

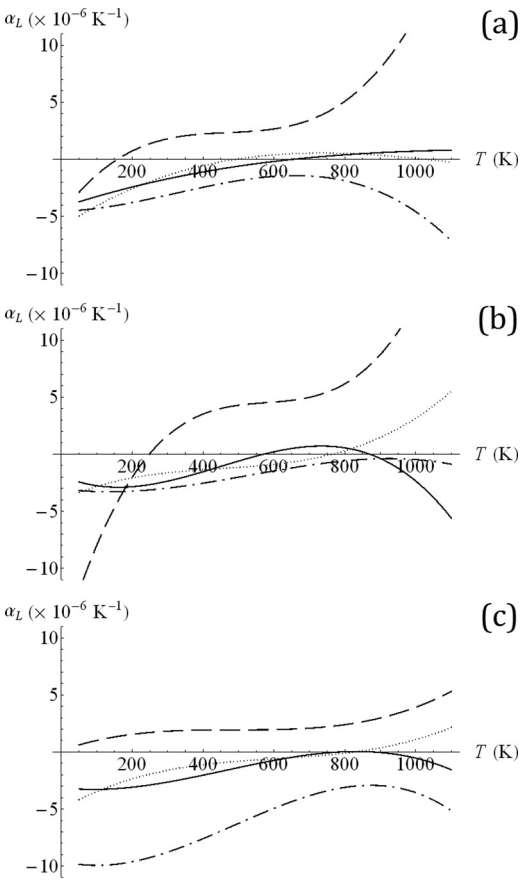

FIG. 4. Average linear TECs of the whole structure of GNMs (full line), their holes (dashed line), and necks (dot-dashed line). The TEC of the corresponding graphene (dotted line) is shown for comparison. (a)–(c) The data for the GNM-46, GNM-62, and GNM-67, respectively.

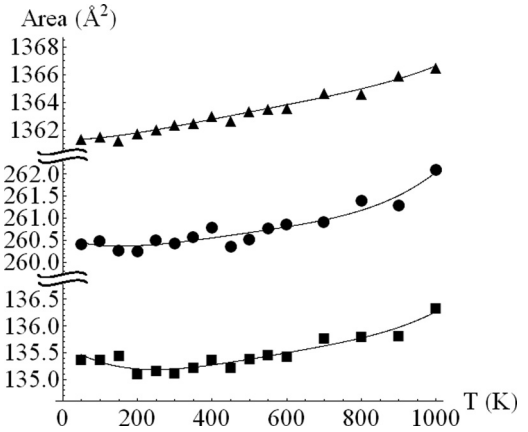

FIG. 5. Area of the holes of the GNM-46 (circle), GNM-62 (square), and GNM-67 (triangle) as functions of the temperature. The full lines are fittings of the points to a fourth order polynomial in T.

The strange behavior of the thermal expansion of the holes can be also observed by computing their areas and plotting them as a function of the equilibrium temperature T. Figure 5 shows the areas of the holes of the three GNMs. Except for low values of temperature, the area of the holes *increases* with temperature, even if the whole structure shrinks.

In terms of the area TECs, the results are similar to those shown in Fig. 4. Figure 6 shows the area TECs of the GNMs, their holes, and the corresponding graphene structures. Area TECs of the holes are positive for most of the values of the temperature considered in this study, and also for most of the values of temperature where the area TEC of the whole GNM structure is negative. This analysis of the area TECs also shows that the behavior of the thermal expansion of the nanoholes in GNMs is contrary to the classical description of the thermal expansion of holes in plates. The differences between the graphene and the whole structure TECs are small, except for large temperatures. The regions in temperature where the area TEC of the hole is negative, for GNM-46 and GNM-62, correspond to the regions in Fig. 5 where the area of their holes decreases with temperature.

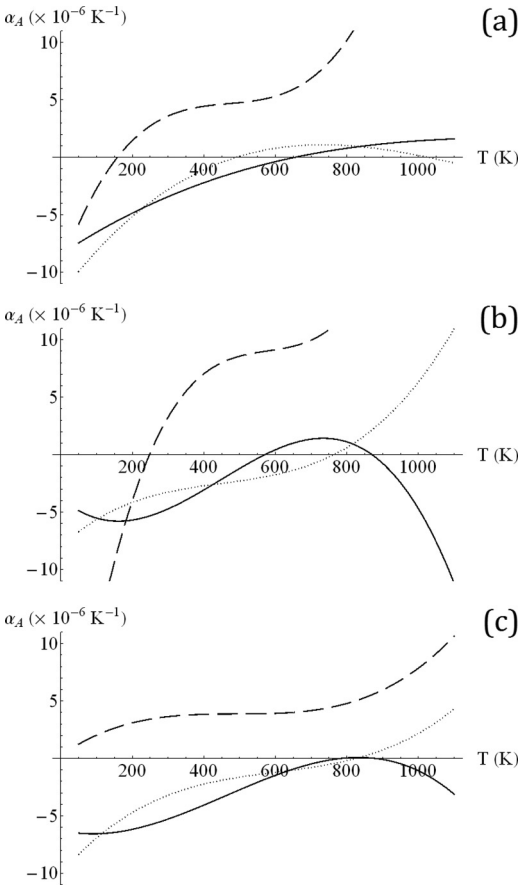

FIG. 6. Area TECs of the whole structure (full line) and its hole (dashed line) of the (a) GNM-46, (b) GNM-62, and (c) GNM-67. The area TECs of the corresponding pristine graphenes (dotted lines) are also shown for comparison.

IV. ANALYSIS OF THE TEC OF GNMS

The following questions arise from the results presented in the previous section. Why, for a certain range of temperatures, is the thermal expansion of the hole contrary (in sign) to the thermal expansion of the whole system? Why are the TEC of the holes different from the TEC of the necks (nonuniformity)? Why is the thermal contraction of the neck region of the GNMs larger than that of the whole structure? How does the neck compensate for the positive thermal expansion of the holes, to provide an overall negative thermal expansion of the GNMs? Is there an explanation for the TEC of the GNMs to be similar to that of the pristine graphene? In order to provide answers to these questions, we performed additional analysis of the structures.

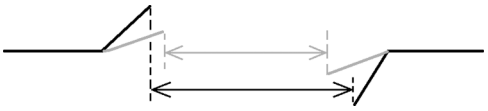

FIG. 8. Scheme proposed to understand the increase of the size of the hole with temperature. Horizontal black lines represent the plane of the GNM and the inclined black and gray lines represent the amplitudes of out-of-plane oscillations of the edges of the hole at large and low temperatures, respectively. Black and gray arrows represent the hole sizes at large and low temperatures, respectively.

First, we make a visual inspection of the displacements of the carbon atoms at regions close and far from the edges of the GNM holes. Figure 7 shows some snapshots of the GNM-67 at different temperatures, where some pieces of the edges of the hole are highlighted to show the amplitude of their displacements along the out-of-plane direction. These images give the impression that the out-of-plane displacements of the carbon atoms close to the hole edges are larger than those of the carbon atoms far from the hole. Similar observations can be made for the other GNM structures (not shown).

From this observation, we propose a qualitative scheme to understand how the size of the hole increases with increasing temperature. As depicted in Fig. 8, the scheme shows that the larger the out-of-plane displacements of the atoms at the edge of the hole, the larger the projection of the free space of the hole onto the x-y plane.

To give quantitative support to this scheme, we computed the time and space averages of the absolute values of the z coordinate $|z|$ of the carbon atoms at two regions: *far from* (here called region I) and *close to* (here called region II) the

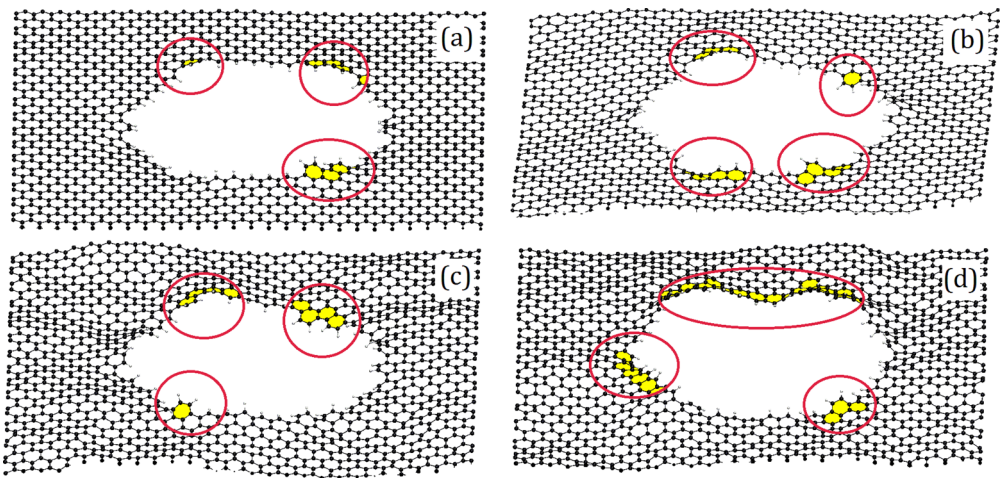

FIG. 7. (Color online) Snapshots of the GNM-67 at (a) 50 K, (b) 300 K, (c) 700 K, and (d) 1000 K. Circles are drawn around some pieces of the structure close to the hole edge (highlighted in yellow) to show their amount of displacement along the out-of-plane direction.

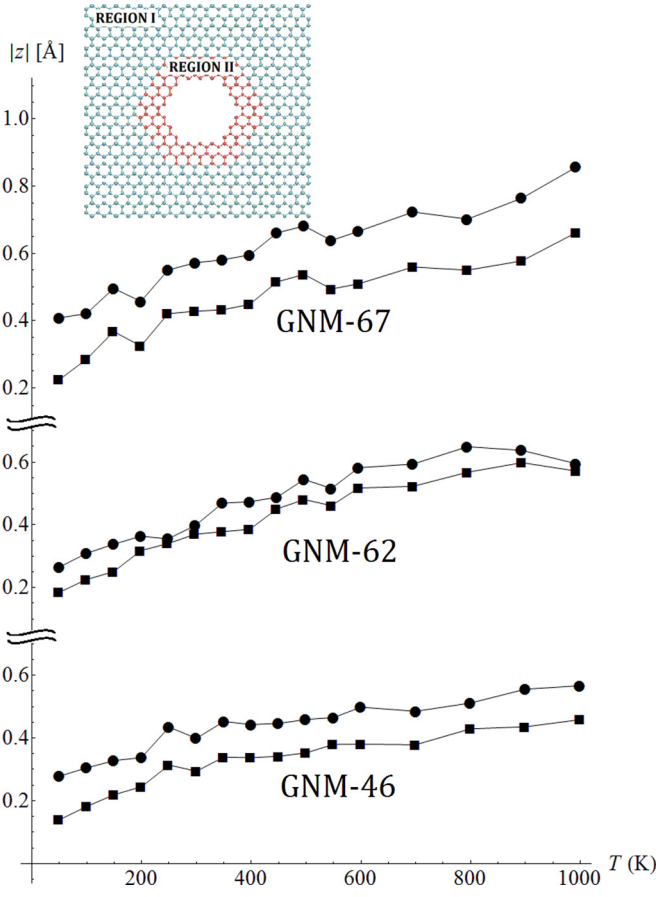

FIG. 9. (Color online) Time and space averages of the absolute values of the z coordinate of the carbon atoms of the GNM-67 (up) GNM-62 (middle), and GNM-46 (bottom) at regions I (square) and II (circle) as defined in the upper-left part of the picture. Circles and squares are values obtained from MD simulations, and full lines are guides to the eyes.

GNM hole. The carbon atoms located at maximum of two lattice parameters away from the hole edge are defined as belonging to region II (or *close to* the hole). Figure 9 shows the average values of the $|z|$ of the carbon atoms of the three GNMs at regions I (squares) and II (circles) as functions of the temperature. For all GNMs, $|z|$ at region II are between $\sim$0.1 and 0.2 Å larger than that at region I. This shows that the displacements along the out-of-plane direction of the carbon atoms close to the hole (region II) are, on average, larger than that of the atoms far from the hole.

Finally, it remains to be understood how the thermal contraction of the neck part of the structure compensates the thermal expansion of the hole in order to provide an overall thermal contraction of the whole GNM structure. Pozzo *et al.* [41] have shown that the negative thermal expansion of free standing graphene comes from in-plane contraction of the graphene lattice parameter a and that this is consistent with the existence of ripples. Here, using the frames from the MD simulations of 200 ps, we calculate the time and space averages of the in-plane lattice parameter a of the regions I and II of the GNM-67 and present the results in Fig. 10. As can be clearly seen, the values of a at region I (far from the hole) are larger than that at region II (close to the hole), showing that the region

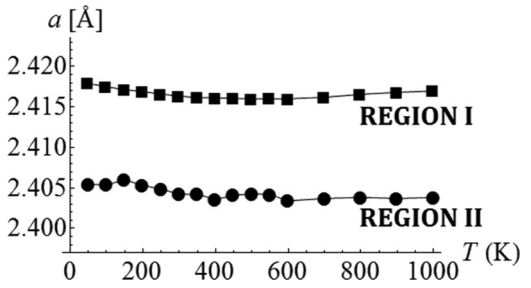

FIG. 10. In-plane lattice parameter of GNM-67 as function of temperature in regions I (square) and II (circle). Circles and squares are values obtained from MD simulations, and full lines are guides to the eyes.

close to the edge of the holes contracts more than the regions far from the edges.

This can be understood in terms of the scheme proposed in Fig. 8. The larger the inclination of the lines close to the edges (inclined black or gray lines in Fig. 8), the smaller the projection of these lines onto the x-y plane. Therefore, as this contraction of the edges is directly related to the expansion of the holes, one compensates the other and the overall thermal expansion of the GNMs should be the same as that of the corresponding pristine graphenes. Figures 4 and 6 show that, except for large temperature, the TECs of the GNMs and corresponding graphene are very close, thus confirming this analysis.

The reason for the thermal expansion of a hole, in a plate, to follow the same trend as that of the material, is the uniformity of the thermal expansion along the plate. As a consequence, the thermal expansion of the full plate will be the same possessing or not holes. Our results suggest that this last statement is more general, in the sense that it does not depend on the uniformity of the thermal expansion of the material. We have seen that, contrary to the behavior of ordinary materials, the thermal expansion of the GNM structure does not occur uniformly. At the region close to the hole edges (region II), the thermal expansion is larger than that at regions far from the hole (region I). However, because the reason for the expansion of the hole in the GNMs is also the reason for the contraction of the region I (close to the edges), the thermal expansion of the whole structure was observed to be the same as if there were no holes.

V. CONCLUSIONS

In summary, our numerical experiments have revealed an interesting phenomenon regarding the thermal expansion behavior of holes in GNMs. We have observed that, at certain ranges of temperature, the hole of a GNM expands (contracts) while the whole structure contracts (expands). This behavior is contrary to the classical prediction for the thermal expansion of holes, that is to be the same as the thermal expansion of the whole material. Also, the thermal expansion of the neck was observed to be always smaller than that of the whole structure of the GNM, what is also different from the classical prediction which says that the thermal expansion of the neck should be uniform and equal to that of the material.

Here we showed that not only is the thermal expansion of GNMs not uniform along the structure, but also that this nonuniformity explains the unexpected thermal expansion behavior of holes in GNMs. This is confirmed by the analysis of the magnitude of displacements along the out-of-plane direction of the atoms close to the edge of the hole. It was shown that they are larger than that of the atoms far from the hole. A simple scheme was proposed to help understand that larger the out-of-plane displacements of these atoms, due to thermal excitation, the larger (smaller) the projected size of the holes (of the regions close to the edges) onto the plane of the GNM. The calculation of the in-plane lattice parameter along the structure confirms the above results because it was shown to be smaller at the regions close to the hole edges than that far from the holes.

Although the unexpectedness of the thermal expansion behavior of the holes in GNMs, the thermal expansion of the GNMs was observed to be approximately equal to the thermal expansion of the corresponding graphenes. This can also be understood in terms of our proposed scheme which shows that the expansion of the hole is compensated by the contraction of the regions close to the edges. This suggests that the classical prediction that the thermal expansion of plates with or without holes are the same does not depend on the uniformity of the thermal expansion of the material along the structure.

Several types of applications have been suggested for GNMs and this unexpected thermal expansion of the holes can be useful to predict the behavior of combined GNM and other systems under thermal excitation (like in the proposed application of GNMs to DNA sequencing [27]). One interesting question is about the possible dependence of this unusual behavior on the thickness of the structure. We hope our results can further motivate new studies on applications of GNMs as well as to reveal new thermal and mechanical phenomena.

ACKNOWLEDGMENTS

This work was supported in part by the Brazilian Agencies CNPq, FAPESP, FAPERJ, and FAEPEX/UNICAMP. A.F.F. acknowledges Grant No. 2012/10106-8 from São Paulo Research Foundation (FAPESP).

[1] D. Halliday, R. Resnick, and J. Walker, *Fundamentals of Physics*, 6th ed. (John Wiley and Sons, New York, 2001).
[2] S. Cuenot, C. Frétigny, S. Demoustier-Champagne, and B. Nysten, Phys. Rev. B **69**, 165410 (2004).
[3] Y. Tang and M. Ouyang, Nat. Mater. **6**, 754 (2007).
[4] L. D. Machado, S. B. Legoas, J. S. Soares, N. Shadmi, A. Jorio, E. Joselevich, and D. S. Galvao, Phys. Rev. Lett. **110**, 105502 (2013).
[5] L. J. Hall, V. R. Coluci, D. S. Galvao, M. E. Kozlov, M. Zhang, S. O. Dantas, and R. H. Baughman, Science **320**, 504 (2008).
[6] E. Perim, A. F. Fonseca, N. M. Pugno, and D. S. Galvao, Europhys. Lett. **105**, 56002 (2014).
[7] A. A. Balandin, Nat. Mater. **10**, 569 (2011).
[8] W. Bao, F. Miao, Z. Chen, H. Zhang, W. Jang, C. Dames, and C. Ning Lau, Nat. Nanotechnol. **4**, 562 (2009).
[9] V. Singh, S. Sengupta, H. S. Solanki, R. Dhall, A. Allain, S. Dhara, P. Pant, and M. M. Deshmukh, Nanotechnology **21**, 165204 (2010).
[10] D. Yoon, Y.-W. Son, and H. Cheong, Nano Lett. **11**, 3227 (2011).
[11] K. S. Novoselov, A. K. Geim, S. V. Morozov, D. Jiang, Y. Zhang, S. V. Dubonos, I. V. Grigorieva, and A. A. Firsov, Science **306**, 666 (2004).
[12] K. S. Novoselov, D. Jiang, F. Schedin, T. J. Booth, V. V. Khotkevich, S. V. Morozov, and A. K. Geim, Proc. Natl. Acad. Sci. U.S.A. **102**, 10451 (2005).
[13] A. H. Castro Neto, F. Guinea, N. M. R. Peres, K. S. Novoselov, and A. K. Geim, Rev. Mod. Phys. **81**, 109 (2009).
[14] R. S. Edwards and K. S. Coleman, Nanoscale **5**, 38 (2013).
[15] C. Berger, Z. Song, X. Li, X. Wu, N. Brown, C. Naud, D. Mayou, T. Li, J. Hass, A. N. Marchenkov, E. H. Conrad, P. N. First, and W. A. de Heer, Science **312**, 1191 (2006).
[16] M. Y. Han, B. Ozyilmaz, Y. Zhang, and P. Kim, Phys. Rev. Lett. **98**, 206805 (2007).
[17] R. Balog, B. Jørgensen, L. Nilsson, M. Andersen, E. Rienks, M. Bianchi, M. Fanetti, E. Lægsgaard, A. Baraldi, S. Lizzit, Z. Sljivancanin, F. Besenbacher, B. Hammer, T. G. Pedersen, P. Hofmann, and L. Hornekær, Nat. Mater. **9**, 315 (2010).
[18] S. Park and R. S. Ruoff, Nature Nanotechnology **4**, 217 (2009).
[19] J. Bai, X. Zhong, S. Jiang, Y. Huang, and X. Duan, Nat. Nanotechnol. **5**, 190 (2010).
[20] A. Sinitskii and J. M. Tour, J. Am. Chem. Soc. **132**, 14730 (2010).
[21] L. Zhang, S. Diao, Y. Nie, K. Yan, N. Liu, B. Dai, Q. Xie, A. Reina, J. Kong, and Z. Liu, J. Am. Chem. Soc. **133**, 2706 (2011).
[22] O. Akhavan, ACS Nano **4**, 4174 (2010).
[23] G. Ning, Z. Fan, G. Wang, J. Gao, W. Qianc, and F. Wei, Chem. Commun. **47**, 5976 (2011).
[24] L. Liu, Y. Zhang, W. Wang, C. Gu, X. Bai, and E. Wang, Adv. Mater. **23**, 1246 (2011).
[25] X. Wang, L. Jiao, K. Sheng, C. Li, L. Dai, and G. Shi, Sci. Rep. **3**, 1996 (2013).
[26] P. T. Xu, J. X. Yang, K. S. Wang, Z. Zhou, and P. W. Shen, Chin. Sci. Bull. **57**, 2948 (2012).
[27] A. Girdhara, C. Satheb, K. Schultena, and J.-P. Leburton, Proc. Natl. Acad. Sci. U.S.A. **110**, 16748 (2013).
[28] A. Esfandiar, N. J. Kybert, E. N. Dattoli, G. H. Han, M. B. Lerner, O. Akhavan, A. Irajizad, and A. T. C. Johnson, Appl. Phys. Lett. **103**, 183110 (2013).
[29] O. Akhavan and E. Ghaderi, Small **9**, 3593 (2013).
[30] S. Jungthawan, P. Reunchan, and S. Limpijumnong, Carbon **54**, 359 (2013).
[31] R. Sako, N. Hasegawa, H. Tsuchiya, and M. Ogawa, J. Appl. Phys. **113**, 143702 (2013).
[32] H. Şahin, and S. Ciraci, Phys. Rev. B **84**, 035452 (2011).
[33] R. Petersen, T. G. Pedersen, and A.-P. Jauho, ACS Nano **5**, 523 (2011).
[34] I. I. Naumov and A. M. Bratkovsky, Phys. Rev. B **85**, 201414(R) (2012).
[35] Y. J. Sun, F. Ma, and K. W. Xu, Integrated Ferroelectrics **128**, 118 (2011).

[36] N. C. B. Mostério, and A. F. Fonseca, MRS Proc. **1505**, opl.2013.186 (2013).
[37] C. Carpenter, A. M. Christmann, L. Hu, I. Fampiou, A. R. Muniz, A. Ramasubramaniam, and D. Maroudas, Appl. Phys. Lett. **104**, 141911 (2014).
[38] T. Gunst, T. Markussen, A.-P. Jauho, and M. Brandbyge, Phys. Rev. B **84**, 155449 (2011).
[39] In fact, in Ref. [36] we have performed initial calculations to estimate the thermal expansion coefficient of some GNMs, but have not done any detailed analysis of the thermal expansion of the holes.
[40] N. Mounet and N. Marzari, Phys. Rev. B **71**, 205214 (2005).
[41] M. Pozzo, D. Alfè, P. Lacovig, P. Hofmann, S. Lizzit, and A. Baraldi, Phys. Rev. Lett. **106**, 135501 (2011).
[42] P. K. Schelling and P. Keblinski, Phys. Rev. B **68**, 035425 (2003).
[43] P. L. de Andres, F. Guinea, and M. I. Katsnelson, Phys. Rev. B **86**, 144103 (2012).
[44] Large-scale Atomic/Molecular Massively Parallel Simulator. http://lammps.sandia.gov
[45] S. Plimpton, J. Comput. Phys. **117**, 1 (1995).
[46] D. W. Brenner, O. A. Shenderova, J. A. Harrison, S. J. Stuart, B. Ni, and S. B. Sinnot, J. Phys.: Condens. Matter **14**, 783 (2002).
[47] B. I. Yakobson, C. J. Brabec, and J. Bernholc, Phys. Rev. Lett. **76**, 2511 (1996).
[48] O. A. Shenderova, D. W. Brenner, A. Omeltchenko, X. Su, and L. H. Yang, Phys. Rev. B **61**, 3877 (2000).
[49] C. Wei, D. Srivastava, and K. Cho, Nano Lett. **2**, 647 (2002).
[50] D. Srivastava, C. Wei, and K. Cho, Appl. Mech. Rev. **56**, 215 (2003).
[51] V. R. Coluci, N. M. Pugno, S. O. Dantas, D. S. Galvao, and A. Jorio, Nanotechnology **18**, 335702 (2007).
[52] F. de Brito Mota, E. F. Almeida, Jr., and C. M. C. de Castilho, Braz. J. Phys. **38**, 70 (2008).
[53] M. Neek-Amal and F. M. Peeters, Phys. Rev. B **83**, 235437 (2011).
[54] H. Jiang, B. Liu, Y. Huang, and K. C. Hwang, J. Eng. Mater. Technol. **126**, 265 (2004).
[55] K. V. Zakharchenko, M. I. Katsnelson, and A. Fasolino, Phys. Rev. Lett. **102**, 046808 (2009).
[56] Although the area of the hole could be a more complex function of $h_x \times h_y$, the corresponding area TEC would not. It could be defined a constant parameter γ where the exact area of the hole is equal to $\gamma \times (h_x \times h_y)$ (if the hole has a shape of an ellipse, $\gamma = \pi/4$). But as γ does not depend on T, in Eq. (1) it will be canceled out and the area TEC will not depend on γ.
[57] J.-W. Jiang, J.-S. Wang, and B. Li, Phys. Rev. B **80**, 205429 (2009).